nature biotechnology

Optogenetic control of endogenous Ca^{2+} channels *in vivo*

Taeyoon Kyung[1,7], Sangkyu Lee[2,7], Jung Eun Kim[1], Taesup Cho[2], Hyerim Park[1], Yun-Mi Jeong[3], Dongkyu Kim[1], Anna Shin[1], Sungsoo Kim[1], Jinhee Baek[2,4], Jihoon Kim[1], Na Yeon Kim[1], Doyeon Woo[1], Sujin Chae[5], Cheol-Hee Kim[3], Hee-Sup Shin[2,4], Yong-Mahn Han[1], Daesoo Kim[1] & Won Do Heo[1,2,5,6]

Calcium (Ca^{2+}) signals that are precisely modulated in space and time mediate a myriad of cellular processes, including contraction, excitation, growth, differentiation and apoptosis[1]. However, study of Ca^{2+} responses has been hampered by technological limitations of existing Ca^{2+}-modulating tools. Here we present OptoSTIM1, an optogenetic tool for manipulating intracellular Ca^{2+} levels through activation of Ca^{2+}-selective endogenous Ca^{2+} release–activated Ca^{2+} (CRAC) channels. Using OptoSTIM1, which combines a plant photoreceptor[2,3] and the CRAC channel regulator STIM1 (ref. 4), we quantitatively and qualitatively controlled intracellular Ca^{2+} levels in various biological systems, including zebrafish embryos and human embryonic stem cells. We demonstrate that activating OptoSTIM1 in the CA1 hippocampal region of mice selectively reinforced contextual memory formation. The broad utility of OptoSTIM1 will expand our mechanistic understanding of numerous Ca^{2+}-associated processes and facilitate screening for drug candidates that antagonize Ca^{2+} signals.

Ca^{2+} signals are generated through the concerted action of numerous ion channels, pumps and receptors on intracellular Ca^{2+} stores, such as the endoplasmic reticulum, and on the plasma membrane[1]. These signals can be encoded as distinct patterns with varying amplitude, frequency or duration, ranging from microseconds to hours. There have been several attempts to directly induce intracellular Ca^{2+} signals to study their impact on specific cellular functions. Of the approaches for generating various patterns of Ca^{2+} signals with controlled onset time, methods based on chemical modulators such as Ca^{2+} mobilizers and receptor ligands have been the most widely used. However, these approaches lack reversibility and spatial precision. 'Caged' compounds[5] that can be photolytically converted to free Ca^{2+} or Ca^{2+}-inducing chemicals enable reversible control of intracellular Ca^{2+} levels with high spatial resolution. However, they release byproducts (i.e., protecting groups) after photolysis, cause local depletion of caged molecules upon prolonged stimulation, and are impractical for application *in vivo*. Optogenetics approaches[6] are free of these limitations. Optogenetic tools, such as variants of the nonselective cation channel channelrhodopsin (ChR)[6], enable control of the electrical activity of a particular sub-population of cells. Recently, two optogenetic tools, PACR and LOVS1K, exploiting LOV2 domain of phototropin receptor to generate a 'caged protein' have been used to control intracellular Ca^{2+} levels ($[Ca^{2+}]_i$)[7,8]. However, PACR, which controls Ca^{2+}-binding affinity of calmodulin-M13 peptide, has a low dynamic range ($\Delta[Ca^{2+}]_i$ of ~90 nM)[7], which is insufficient to reach the physiologically active dynamic range of intracellular Ca^{2+} (100–1,000 nM). LOVS1K, which controls CRAC channel activity by releasing an active STIM1 fragment, requires exogenous coexpression of Orai1 (pore-forming subunit of CRAC channel) to mediate Ca^{2+} influx[8].

Here we present a single-component optogenetic module that allows specific control of intracellular Ca^{2+} levels through activation of ubiquitously expressed endogenous CRAC channels. We designed an array of synthetic proteins in which the PHR domain[2,3] of cryptochrome 2 (Cry2) from *Arabidopsis thaliana* is fused to truncated forms of cytosolic STIM1 with potentially varying ability to activate CRAC channels[9,10] (**Supplementary Fig. 1a**). We hypothesized that the light-inducible homo-association property[3] of the Cry2 PHR domain would actively oligomerize STIM1 and translocate to the plasma membrane, where oligomerized STIM1 would bind CRAC channels and trigger Ca^{2+} influx into the cell[4] (**Fig. 1a**).

To test this, we coexpressed each of seven different EGFP-labeled Cry2-STIM1 variants (#1 – #7) with the red-shifted Ca^{2+} indicator, R-GECO1 (ref. 11), in HeLa cells, and exposed them to blue light. Five of the Cry2-STIM1 variants (#1, #3, #4, #6, #7) induced remarkable increases in R-GECO1 fluorescence compared with that of EGFP-Cry2 only (control). In contrast, STIM1 fragments lacking the polybasic domain (K-domain)[9] (#2) or containing a partial deletion of the CRAC channel–activating domain[10] (#5) did not induce a change in $[Ca^{2+}]_i$ (**Supplementary Fig. 1b**). Moreover, conjugation of a light-insensitive Cry2 mutant, Cry2(D387A) (ref. 12) to STIM1 #1 also attenuated the effect on $[Ca^{2+}]_i$ (**Fig. 1b**). The time to reach half-maximal R-GECO1 fluorescence intensity ($Ta_{1/2}$) after activation of Cry2-STIM1 #1 was 64.5 ± 4.8 s (mean ± s.e.m.), whereas $Ta_{1/2}$ values were shorter for Cry2-STIM1 #4 (43.2 ± 3.8 s) and Cry2-STIM1 #7 (48.2 ± 5.4 s), presumably owing to the absence of one of the auto-inhibitory

[1]Department of Biological Sciences, Korea Advanced Institute of Science and Technology (KAIST), Daejeon, Republic of Korea. [2]Center for Cognition and Sociality, Institute for Basic Science (IBS), Daejeon, Republic of Korea. [3]Department of Biology, Chungnam National University, Daejeon, Republic of Korea. [4]Department of Bio and Brain Engineering, KAIST, Daejeon, Republic of Korea. [5]KAIST Institute for the BioCentury, KAIST, Daejeon, Republic of Korea. [6]Cancer Metastasis Control Center, KAIST Institute for the BioCentury, KAIST, Daejeon, Republic of Korea. [7]These authors contributed equally to this work. Correspondence should be addressed to Y.-M.H. (ymhan57@kaist.ac.kr), Daesoo Kim (daesoo@kaist.ac.kr) or W.D.H. (wondo@kaist.ac.kr).

Received 7 May; accepted 20 August; published online 14 September 2015; doi:10.1038/nbt.3350

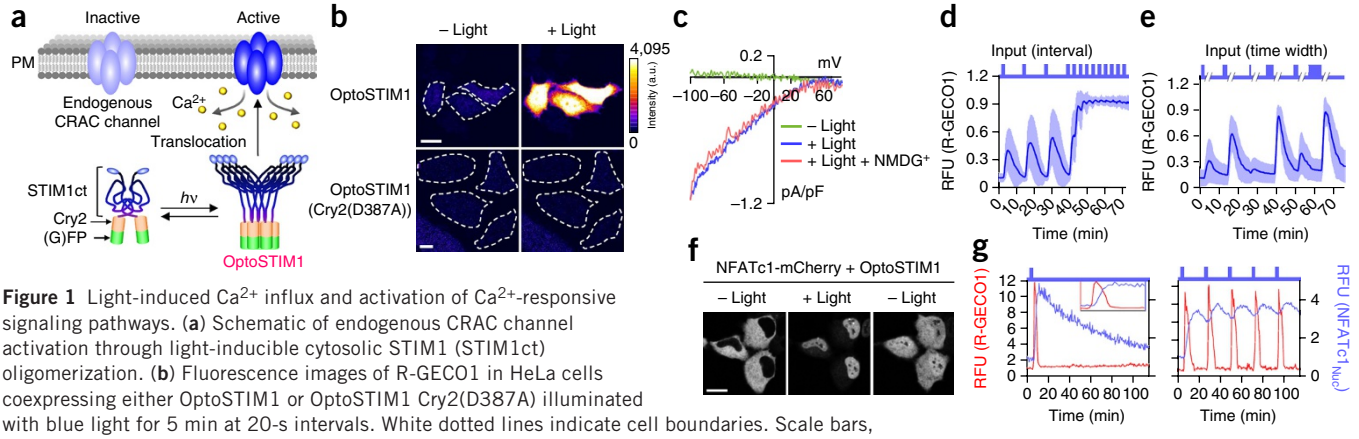

Figure 1 Light-induced Ca^{2+} influx and activation of Ca^{2+}-responsive signaling pathways. (**a**) Schematic of endogenous CRAC channel activation through light-inducible cytosolic STIM1 (STIM1ct) oligomerization. (**b**) Fluorescence images of R-GECO1 in HeLa cells coexpressing either OptoSTIM1 or OptoSTIM1 Cry2(D387A) illuminated with blue light for 5 min at 20-s intervals. White dotted lines indicate cell boundaries. Scale bars, 20 μm. (**c**) Current-voltage (*I-V*) relationships of CRAC currents. HEK293 cells were subjected to whole-cell patch-clamp by ramping membrane potential from −100 mV to +80 mV either before (– light) or during (light) OptoSTIM1 activation. External medium included 10 mM Ca^{2+}, and to assess contribution of Na^+ current, Na^+ in external medium was replaced with $NMDG^+$. (**d**,**e**) Control of Ca^{2+} influx over time by varying stimulation interval (**d**) and duration (**e**). RFU, relative fluorescence intensity of R-GECO1, normalized by the intensity at $t = 0$. Blue lines indicate illumination time points and relative light input values. Power density was fixed at 50 μW mm^{-2}. $n = 24$ (**d**), 26 (**e**) cells. Error bars, s.d. (**f**) Fluorescence images of HeLa cells showing translocation of NFATc1 to the nucleus upon light illumination. Cells were exposed to blue light for 1.5 s. Scale bar, 20 μm. (**g**) Transient or sustained nuclear translocation of NFATc1 by controlling light input (one time or five times at 20-min intervals, respectively) followed by R-GECO1 signal changes. Blue lines indicate light illumination time points.

domains[9] (**Supplementary Fig. 1c**). Notably, we found that the Ca^{2+} influx kinetics was dependent on the expression of Cry2-STIM1 (**Supplementary Fig. 1d**). Given the previous finding that homo-oligomerization kinetics of Cry2 are determined by intracellular Cry2 concentration[13], this result implies that homo-oligomerization process of Cry2-STIM1 is a key determinant for kinetics of CRAC channel activation, in addition to STIM1:Orai1 binding stoichiometry[14]. The deactivation kinetics ($Td_{1/2}$) of Cry2-STIM1 #1, #4 and #7 were 274 ± 23.7 s, 383 ± 52.3 s and 344 ± 34.6 s (mean ± s.e.m.), respectively, indicating that Cry2-STIM1 variants with faster kinetics and higher efficiency in inducing Ca^{2+} increase have a tendency to show slower kinetics of deactivation (**Supplementary Fig. 1e**).

An analysis of subcellular localization with confocal and TIRFM (total internal reflection fluorescence microscopy) imaging revealed that activated Cry2-STIM1 #1, #4, #6, and #7 translocated to the plasma membrane (**Supplementary Fig. 2a**,**b**). This plasma membrane localization of Cry2-STIM1 seems to be indispensable for inducing and stably maintaining Ca^{2+} influx, as dissociation of Cry2-STIM1 from the plasma membrane through rapamycin-mediated FKBP-FRB dimerization was highly correlated with the dramatic decrease of $[Ca^{2+}]_i$ in cells co-expressing EGFP-Cry2-STIM1 #1 with R-GECO1, FKBP-fused anti-GFP nanobody[15], and Tom20-FRB (mitochondria-targeting motif)[16] (**Supplementary Fig. 2c–e**). In addition to plasma membrane localization, Cry2-STIM1 #1 showed dynamic movement along microtubules, through its binding property of microtubule plus end–tracking protein (EB1)[17] (**Supplementary Fig. 3** and **Supplementary Video 1**). In contrast, Cry2-STIM1 #5 and #6 formed abundant clusters upon light illumination, an effect attributable to their propensity to oligomerize[10] in conjunction with Cry2 homo-association. Given the effectiveness of Cry2-STIM1 #1 in increasing Ca^{2+} (**Supplementary Video 2**) and retention of regulatory machinery–binding capacity, we chose Cry2-STIM1 #1 for subsequent experiments and termed it OptoSTIM1.

When we incubated cells co-expressing OptoSTIM1 and R-GECO1 in a medium containing the Ca^{2+}-chelating agent, EGTA, or the Ca^{2+} channel inhibitor, SKF96365, we detected no $[Ca^{2+}]_i$ increase (**Supplementary Fig. 4**). Furthermore, knockdown of Orai1 by small interfering (si)RNA showed dose-dependent attenuation of $[Ca^{2+}]_i$ increase (**Supplementary Fig. 5a–c**) and the expression of dominant-negative Orai1(E106Q)[18] completely blocked Ca^{2+} influx (**Supplementary Fig. 5d**), demonstrating specificity of OptoSTIM1 to endogenous Orai1 channels. Next, to examine OptoSTIM1-bestowed Ca^{2+} selectivity of Orai1 channels based on the previous study describing potential nonselectivity of Orai1 channel for ion current[19], we measured CRAC channel current by whole-cell recording in HEK293 cells. Activated OptoSTIM1 elicited typical inwardly rectifying CRAC channel current, and replacing extracellular Na^+ with $NMDG^+$, an impermeant ion, did not influence the overall amplitude or the shape of CRAC channel current (**Fig. 1c**), reflecting that Na^+ has little or no contribution to OptoSTIM1-mediated CRAC channel current in our system.

To quantitatively control Ca^{2+} influx and measure light-sensitivity of OptoSTIM1, we activated OptoSTIM1 with various light inputs in terms of power density or illumination duration. By varying light power density (10–500 μW mm^{-2}), we found that OptoSTIM1 activity was saturated at 100 μW mm^{-2} (**Supplementary Fig. 6a–c**), where OptoSTIM1 efficiently responded to 457-nm or 488-nm light, but weakly responded or did not respond to the light longer than 514-nm wavelength (**Supplementary Fig. 6d**). This indicated that OptoSTIM1 can be safely combined with red-shifted fluorescent indicators. The increased Ca^{2+} level was not further elevated by treatment with thapsigargin, a sarcoplasmic/endoplasmic reticulum calcium ATPase (SERCA) inhibitor that depletes Ca^{2+} in ER lumen and activates endogenous STIM1–Orai1 complexes, suggesting that nearly all functionally available endogenous CRAC channels were occupied and activated by OptoSTIM1 (**Supplementary Fig. 7**). Subsequent treatment of ionomycin further increased R-GECO1 intensity, indicating that the capacity of R-GECO1 was not saturated. Increasing duration of light input (0.5–4.5 s) at modest power density (10 μW mm^{-2}) produced Ca^{2+} transients with elevated amplitudes (**Supplementary Fig. 8**). Pulsatile illumination at 10- and 3-min intervals induced transient and sustained $[Ca^{2+}]_i$ increases, respectively (**Fig. 1d** and **Supplementary Video 3**), and changing the duration of light inputs at fixed time interval dynamically controlled intracellular

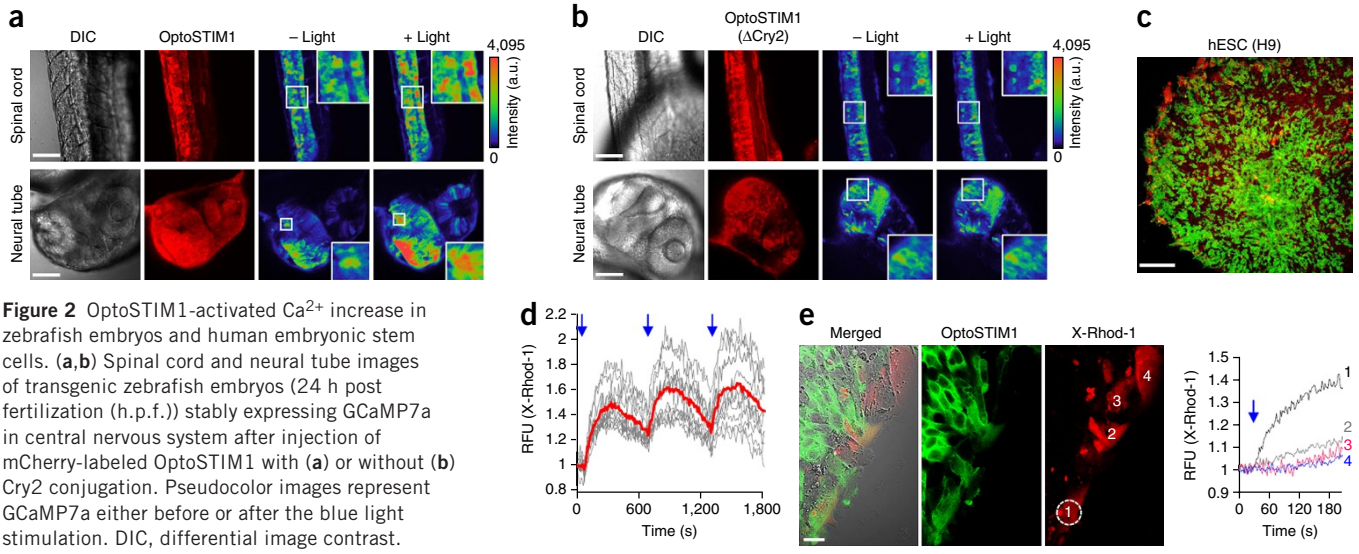

Figure 2 OptoSTIM1-activated Ca^{2+} increase in zebrafish embryos and human embryonic stem cells. (**a**,**b**) Spinal cord and neural tube images of transgenic zebrafish embryos (24 h post fertilization (h.p.f.)) stably expressing GCaMP7a in central nervous system after injection of mCherry-labeled OptoSTIM1 with (**a**) or without (**b**) Cry2 conjugation. Pseudocolor images represent GCaMP7a either before or after the blue light stimulation. DIC, differential image contrast. Scale bars, 50 µm. (**c**) Merged fluorescence image of H9 hESC line stably expressing OptoSTIM1. Green and red fluorescence indicate OptoSTIM1 and X-Rhod-1, respectively. Scale bar, 200 µm. (**d**) Reversible increases of Ca^{2+} in hESCs induced by repeatable OptoSTIM1 activation. Gray lines indicate signal changes of X-Rhod-1 in each individual cell ($n = 12$). The red line indicates the averaged signal change. Blue arrows indicate time points of light illumination given at 10-min intervals. (**e**) Spatial illumination of a small region of an hESC colony. White dotted circle indicates the light stimulation region. Scale bar, 20 µm. Graph on the right shows relative changes in X-Rhod-1 intensity upon blue light illumination. The blue arrow indicates the time point of light input.

Ca^{2+} concentration (**Fig. 1e**). Notably, OptoSTIM1 could be stably and repeatedly activated at least 20 times during 300 min, with some extent of cell-to-cell or pulse-to-pulse variation (**Supplementary Fig. 9**).

Next, we examined whether OptoSTIM1 expression has an effect on basal $[Ca^{2+}]_i$ together with the two other recently developed intracellular Ca^{2+}-elevating tools, LOVS1K and PACR. Ratiometric imaging with Fura-2 indicated that resting $[Ca^{2+}]_i$ has a positive correlation with the expression level of OptoSTIM1 (**Supplementary Fig. 10a**). LOVS1K also exhibited this tendency, but when co-expressed with Orai1, the basal $[Ca^{2+}]_i$ showed a bell-shaped distribution as a function of LOVS1K:Orai1 expression ratio, implying that certain ratios (0.6–0.9) of their expression induced constitutive activation of CRAC channels regardless of light illumination. In contrast, PACR induced no elevation in basal $[Ca^{2+}]_i$; rather the expression level of PACR negatively correlated with basal $[Ca^{2+}]_i$, reflecting that PACR captured cytosolic free Ca^{2+} and resulted in basal $[Ca^{2+}]_i$ decrease. Despite the increase of basal $[Ca^{2+}]_i$ compared to that of control in OptoSTIM1-expressing cells, levels in most cells were within the range of physiologically relevant resting $[Ca^{2+}]_i$ (~100 nM)[1]. Moderate or low expression level of OptoSTIM1 (~65% of total cells) had no effect on basal $[Ca^{2+}]_i$, compared to that of nontransfected cells (**Supplementary Fig. 10a**,**b**), and $[Ca^{2+}]_i$ in these subpopulation of cells reached ~500 nM upon light illumination (**Supplementary Fig. 10c**). To determine whether OptoSTIM1 in the subgroup of cells retains functionality in terms of Ca^{2+}-responsive downstream pathway, we measured phosphorylation of endogenous CREB (cAMP-responsive element-binding) protein. In the dark state, OptoSTIM1-expressing cells within the threshold had no substantial effect in the level of pCREB relative to that of non-expressing cells (**Supplementary Fig. 10d**,**e**). However, light illumination resulted in a remarkable increase of CREB phosphorylation, demonstrating functionality of OptoSTIM1 without perturbation on basal $[Ca^{2+}]_i$.

To compare efficiency of inducing $[Ca^{2+}]_i$ increase by OptoSTIM1 and LOVS1K, which target the same Ca^{2+} channel, we introduced OptoSTIM1 or LOVS1K in the presence or absence of Orai1 into various cell types. In fibroblasts, endothelial or excitable cells, OptoSTIM1 triggered notable, yet varied, levels of Ca^{2+} influx upon light illumination (**Supplementary Fig. 11a**,**b**), partly explained by varied levels of Orai1 mRNA among different cell types and the previous finding of STIM1:Orai1 ratio–dependent regulation of Orai1 channel activity[14] (**Supplementary Fig. 11c**). Notably, LOVS1K alone triggered weak or no Ca^{2+} influx in the same illuminating condition. In HeLa cells, LOVS1K raised the intensity of G-GECO1.0 (Ca^{2+} indicator) ~1.7-fold, and only less than 10% of LOVS1K-expressing cells responded to blue light more strongly, demonstrated by the large value of coefficient of variation. However, almost all cells with OptoSTIM1 showed over tenfold $[Ca^{2+}]$ increase (**Supplementary Figs. 11a**,**b** and **12a**). Moreover, neither NIH3T3 cells nor human umbilical vein endothelial cells expressing LOVS1K responded to blue light even in the presence of coexpressed Orai1, suggesting that OptoSTIM1 offers more extensive applicability and substantially higher efficiency of inducing Ca^{2+} influx compared to LOVS1K. PACR, despite faster kinetics in elevating Ca^{2+} ($1/k_{off}$ = 5.54 ms)[7] compared to that of OptoSTIM1 ($Ta_{1/2}$ = 64.5 ± 4.8 s) or LOVS1K ($Ta_{1/2}$ = 50 ± 5.2 s; **Supplementary Figs. 1c** and **12b**), exhibited incomparably low dynamic range (~8%) detected with R-GECO1, and required 1.5 s of 1 mW mm^{-2} (488 nm) for saturated activity, which is a tenfold higher light power density compared to that of OptoSTIM1 (**Supplementary Fig. 13**).

We next applied OptoSTIM1 to tunable control of Ca^{2+} signaling pathways. Nuclear factor of activated T cells (NFAT) are a family of Ca^{2+}-responsive transcription factors that translocate to the nucleus and participate in regulating the expression of numerous genes[20]. Brief activation of OptoSTIM1 caused rapid (<5 min) translocation of NFAT, cytoplasmic, calcineurin-dependent 1 (NFATc1)-mCherry to the nucleus followed by a slow return to the cytoplasm (~100 min), even after $[Ca^{2+}]_i$ returned to basal levels, consistent with the previous finding that NFAT functions as a working memory[20] of Ca^{2+} (**Fig. 1f**,**g** and **Supplementary Video 4**). By contrast, five transient increases in $[Ca^{2+}]_i$ induced by pulsatile illumination at 20-min intervals resulted in sustained NFATc1 residence in the nucleus (**Fig. 1g**).

Other major cellular effects of Ca^{2+} include actin reorganization and changes in cell morphology[21]. Transient activation of OptoSTIM1

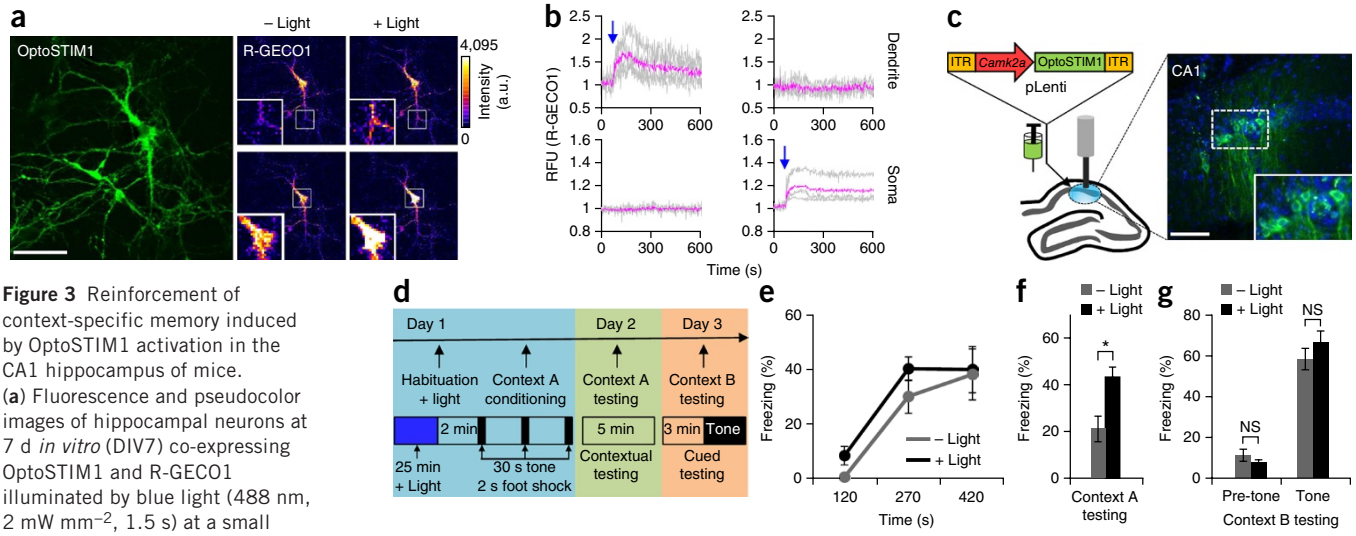

Figure 3 Reinforcement of context-specific memory induced by OptoSTIM1 activation in the CA1 hippocampus of mice. (**a**) Fluorescence and pseudocolor images of hippocampal neurons at 7 d *in vitro* (DIV7) co-expressing OptoSTIM1 and R-GECO1 illuminated by blue light (488 nm, 2 mW mm^{-2}, 1.5 s) at a small region of the dendrite or soma. pLenti, lentiviral expression plasmid. Scale bar, 50 µm. (**b**) Changes in R-GECO1 fluorescence intensity over time in dendrites ($n = 4$) and soma ($n = 3$) upon light illumination. Blue arrows indicate time points of light illumination. Magenta lines represent average values of R-GECO1 fluorescence intensity. (**c**) Schematic representation showing stimulation of the *Camk2a* promoter–driven OptoSTIM1 lentivirus-infected CA1 region (blue) of the hippocampus through an optic fiber. Representative image showing expression of OptoSTIM1 in the CA1 region of a mouse. Blue, DAPI; green, OptoSTIM1. Scale bar, 50 µm. (**d**) Basic scheme for behavior experiments. Mice were illuminated (blue box) in their home cage before fear conditioning (black boxes in day 1). A foot shock was applied for 2 s at the end of each 30-s tone. Contextual and auditory cued fear memories were tested 24 h and 48 h after training, respectively. (**e**–**g**) Percentage of freezing behavior of mice at given time points during fear conditioning (**e**), at 24 h after training in the same context (**f**), and at 48 h after training in a novel context (**g**). *$P = 0.00255$ for illuminated ($n = 9$) versus non-illuminated ($n = 6$); NS, not significant by Student's two-tailed *t*-test. Error bars, s.e.m.

induced reversible F-actin disassembly at the cell cortex, monitored by iRFP670-labeled Lifeact (F-actin probe)[22,23] (**Supplementary Fig. 14a–d** and **Supplementary Video 5**). This effect was attenuated by treatment with SKF96365 or expression of OptoSTIM1 without Cry2, even under light illumination (**Supplementary Fig. 14e**). In morphologically dynamic NIH3T3 fibroblasts, protruded membrane structures were reversibly retracted at the plasma membrane upon blue light (**Supplementary Fig. 14f**). These results demonstrate that OptoSTIM1-induced Ca^{2+} influx can remodel actin cytoskeleton structure.

Next, we explored whether OptoSTIM1 can induce Ca^{2+} influx *in vivo* by injecting OptoSTIM1 RNA into zebrafish embryos stably expressing genetically encoded Ca^{2+} indicator, GCaMP7a[24], in the central nervous system. Upon photoexcitation, GCaMP7a fluorescence intensity was increased in neural tubes and spinal cords but not in Cry2-lacking OptoSTIM1 (OptoSTIM1 (ΔCry2)) injected embryos (**Fig. 2a**,**b**), demonstrating functionality of OptoSTIM1 *in vivo*.

Ca^{2+} signaling has an essential role in stem cell proliferation and differentiation, but the function of Ca^{2+} signals in undifferentiated human embryonic stem cells (hESCs) is poorly understood[25]. To examine the functional expression of endogenous CRAC channels in pluripotent stem cells, we targeted H9 cells, a widely used hESC line, with a lentivirus expressing OptoSTIM1 under the control of an *Ef1α* promoter, and monitored Ca^{2+} signals with the Ca^{2+} indicator, X-Rhod-1 (**Fig. 2c**). Light illumination induced rapid and reversible Ca^{2+} increases in hESC colonies (**Fig. 2d** and **Supplementary Fig. 15**). Based on the spatial resolution of OptoSTIM1 in a population level (**Supplementary Fig. 16a** and **Supplementary Video 6**) and a subcellular level (**Supplementary Fig. 16b**) of HeLa cells, we selectively irradiated blue light on a single cell in a hESC colony. Notably, cells in distant and non-illuminated regions also exhibited Ca^{2+} responses with delayed kinetics, suggesting Ca^{2+}-mediated cell-cell communication possibly through gap junctions[26] in hESC aggregates (**Fig. 2e**).

Recently, roles of neuronal store-operated Ca^{2+} entry (SOCE) primarily mediated by STIM1 or STIM2 have been described in cerebellar, hippocampal and cortical neurons[27]. In cultured hippocampal neurons transiently expressing OptoSTIM1 and R-GECO1, pulsatile illuminations of blue light rapidly triggered Ca^{2+} influx (**Supplementary Fig. 17**), which could be selectively controlled in dendrites or soma (**Fig. 3a**,**b**) and was substantially attenuated by SKF96365 treatment (**Supplementary Fig. 18**). By contrast, LOVS1K by itself could not trigger Ca^{2+} increase (**Supplementary Fig. 19**), further supporting the extensive applicability of OptoSTIM1. We next tested whether OptoSTIM1-induced Ca^{2+} influx in the hippocampus affected the process of memory formation and subsequent behavior in mice. We targeted the CA1 region of the hippocampus of wild-type mice with an OptoSTIM1 lentivirus under the control of a Ca^{2+}/calmodulin-dependent protein kinase IIα (*Camk2a*) promoter, selective for excitatory neurons, and implanted with an optical fiber (**Fig. 3c**). Because it is known that contextual, but not auditory-cued, fear memory relies on the hippocampus[28], we tested both types of memory in these mice. For this, on day 1, we delivered optic fiber–mediated blue light for 25 min to the mice, and placed the mice in a conditioning chamber (context A) to receive paired stimuli of a tone (30 s, 90 dB, 3 kHz) and a co-terminating foot shock (2 s, 0.7 mA) (**Fig. 3d**). During three tone-shock pairings of conditioning, we observed comparable efficiencies of freezing behavior in OptoSTIM1-expressing mice either light-illuminated or not (**Fig. 3e**). However, on day 2, placing mice into the same chamber where they underwent pairings of tone shock aroused fear, and notably OptoSTIM1-stimulated mice exhibited approximately a twofold increase in time dedicated to freezing behavior compared to that of non-irradiated mice, implying the increase in contextual fear memory in OptoSTIM1-stimulated mice (**Fig. 3f**). We could not detect any significant difference in freezing behavior between mice with light-illumination and those without light exposure in response to auditory cues on day 3 (**Fig. 3g**), demonstrating that OptoSTIM1 activation

in hippocampus selectively reinforced contextual but not auditory memory. This result also suggests that there might be reinforcing roles of specific Ca^{2+} signals in the contextual memory-encoding process even before onset of the learning event, which is independent of action potential firing in CA1 hippocampal neurons where ChR2 induced bursts of action potentials in the same experimental condition (**Supplementary Fig. 20**).

In this study, we described a single-component optogenetic module, OptoSTIM1, that can reversibly and quantitatively modulate intracellular Ca^{2+} levels through Ca^{2+} selectivity–bestowed endogenous CRAC channels with spatiotemporal precision, and showed that the resulting Ca^{2+} signals can be decoded by Ca^{2+}-responsive signaling molecules. We also found out that contrary to physiological stimulation of CRAC channels via full-length STIM1, which occurs in ER–plasma membrane junctions, OptoSTIM1 activates all plasma membrane–localized CRAC channels that are functionally available. The advantages of OptoSTIM1 over previously developed tools, PACR and LOVS1K, are high dynamic range of Ca^{2+} increase and direct control of endogenous CRAC channels in various cell types and *in vivo* models. We also demonstrated OptoSTIM1-induced Ca^{2+} influx in hESCs and suggested a potential mechanism for Ca^{2+}-mediated signal propagation among hESCs in a colony. A notable finding was the ability of OptoSTIM1 to enhance the learning capacity of mice. Because we stimulated OptoSTIM1 in the CA1 region of the hippocampus before the process of memory formation, the increase in contextual fear memory in light-illuminated mice provides evidence for the existence of mechanism that reinforces memory formation through non-associative Ca^{2+}. This might be explained by changes in the activities of several well-characterized Ca^{2+}-responsive proteins, such as Ca^{2+}/calmodulin-dependent kinases (CaMKs) and cAMP response element-binding (CREB) protein[29]. Given the evidence that abnormal CRAC channel activity is involved in human diseases[30], OptoSTIM1 will enable robust cell- or animal-based screening for identifying drug candidates that target CRAC channels.

Despite its usefulness, OptoSTIM1 may encounter several challenges to overcome. Utilizing the full cytosolic region of STIM1 may result in unintentional perturbation of cell physiology, owing to binding partners working apart from CRAC channel regulation[4]. This complexity could be partially simplified by using chemical modulators and/or truncated or mutated forms of STIM1 with a distinct set of interactors. Moreover, Ca^{2+} entry through the plasma membrane by OptoSTIM1 restricts its applicability to selectively control $[Ca^{2+}]_i$ in other cellular compartments such as the nucleus. Slower action kinetics of OptoSTIM1 compared to that of PACR might be overcome by using other photoreceptors or engineered Cry2 with faster kinetics. Finally, basal $[Ca^{2+}]_i$ increase or heterogeneous Ca^{2+} dynamics owing to high or variable expression of OptoSTIM1 might be relieved by generating stable expression systems or by using weak promoters.

METHODS

Methods and any associated references are available in the online version of the paper.

Note: Any Supplementary Information and Source Data files are available in the online version of the paper.

ACKNOWLEDGMENTS

We thank C.L. Tucker (University of Colorado) for cDNA encoding CRY2PHR-mCherry, T. Inoue (Johns Hopkins University) for cDNA encoding Tom20-FRB, P. Gardner (Stanford University) for cDNA encoding NFATc1-GFP, D. Lee for fruitful discussions and N. Kim for advice on data analysis. This work was supported by the Institute for Basic Science (IBS-R001-G1), the NRF Stem Cell Program (2011-0019509) funded by MSIP, KAIST Institute for the BioCentury, and the National Leading Research Laboratory Program by the Ministry of Science, ICT and Future Planning (2011-0028772 to Daesoo K.), Republic of Korea.

AUTHOR CONTRIBUTIONS

W.D.H., T.K. and S.L. conceived the idea and directed the work. T.K., S.L., J.E.K., T.C., Y.-M.J., J.B., A.S., C.-H.K., H.-S.S., Y.-M.H., Daesoo K. and W.D.H. designed experiments; T.K., S.L., J.E.K., T.C., H.P., Y.-M.J., Dongkyu K., S.K., J.B., A.S., J.K., N.Y.K., D.W. and S.C. performed experiments, and T.K., S.L., Daesoo K. and W.D.H. wrote the manuscript.

COMPETING FINANCIAL INTERESTS

The authors declare no competing financial interests.

1. Berridge, M.J., Lipp, P. & Bootman, M.D. The versatility and universality of calcium signalling. *Nat. Rev. Mol. Cell Biol.* **1**, 11–21 (2000).
2. Kennedy, M.J. *et al.* Rapid blue-light-mediated induction of protein interactions in living cells. *Nat. Methods* **7**, 973–975 (2010).
3. Bugaj, L.J., Choksi, A.T., Mesuda, C.K., Kane, R.S. & Schaffer, D.V. Optogenetic protein clustering and signaling activation in mammalian cells. *Nat. Methods* **10**, 249–252 (2013).
4. Soboloff, J., Rothberg, B.S., Madesh, M. & Gill, D.L. STIM proteins: dynamic calcium signal transducers. *Nat. Rev. Mol. Cell Biol.* **13**, 549–565 (2012).
5. Ellis-Davies, G.C.R. Caged compounds: photorelease technology for control of cellular chemistry and physiology. *Nat. Methods* **4**, 619–628 (2007).
6. Fenno, L., Yizhar, O. & Deisseroth, K. The development and application of optogenetics. *Annu. Rev. Neurosci.* **34**, 389–412 (2011).
7. Fukuda, N., Matsuda, T. & Nagai, T. Optical control of the Ca^{2+} concentration in a live specimen with a genetically encoded Ca^{2+}-releasing molecular tool. *ACS Chem. Biol.* **9**, 1197–1203 (2014).
8. Pham, E., Mils, E. & Truong, K. A synthetic photoactivated protein to generate local or global Ca^{2+} signals. *Chem. Biol.* **18**, 880–890 (2011).
9. Korzeniowski, M.K., Manjarrés, I.M., Varnai, P. & Balla, T. Activation of STIM1-Orai1 involves an intramolecular switching mechanism. *Sci. Signal.* **3**, ra82 (2010).
10. Park, C.Y. *et al.* STIM1 clusters and activates CRAC channels via direct binding of a cytosolic domain to Orai1. *Cell* **136**, 876–890 (2009).
11. Zhao, Y. *et al.* An expanded palette of genetically encoded Ca^{2+} indicators. *Science* **333**, 1888–1891 (2011).
12. Liu, H.T. *et al.* Photoexcited CRY2 interacts with CIB1 to regulate transcription and floral initiation in *Arabidopsis*. *Science* **322**, 1535–1539 (2008).
13. Taslimi, A. *et al.* An optimized optogenetic clustering tool for probing protein interaction and function. *Nat. Commun.* **5**, 4925 (2014).
14. Hoover, P.J. & Lewis, R.S. Stoichiometric requirements for trapping and gating of Ca^{2+} release-activated Ca^{2+} (CRAC) channels by stromal interaction molecule 1 (STIM1). *Proc. Natl. Acad. Sci. USA* **108**, 13299–13304 (2011).
15. Rothbauer, U. *et al.* Targeting and tracing antigens in live cells with fluorescent nanobodies. *Nat. Methods* **3**, 887–889 (2006).
16. Komatsu, T. *et al.* Organelle-specific, rapid induction of molecular activities and membrane tethering. *Nat. Methods* **7**, 206–208 (2010).
17. Grigoriev, I. *et al.* STIM1 is a MT-plus-end-tracking protein involved in remodeling of the ER. *Curr. Biol.* **18**, 177–182 (2008).
18. Vig, M. *et al.* CRACM1 multimers form the ion-selective pore of the CRAC channel. *Curr. Biol.* **16**, 2073–2079 (2006).
19. McNally, B.A., Somasundaram, A., Yamashita, M. & Prakriya, M. Gated regulation of CRAC channel ion selectivity by STIM1. *Nature* **482**, 241–245 (2012).
20. Tomida, T., Hirose, K., Takizawa, A., Shibasaki, F. & Iino, M. NFAT functions as a working memory of Ca^{2+} signals in decoding Ca^{2+} oscillation. *EMBO J.* **22**, 3825–3832 (2003).
21. Prevarskaya, N., Skryma, R. & Shuba, Y. Calcium in tumor metastasis: new roles for known actors. *Nat. Rev. Cancer* **11**, 609–618 (2011).
22. Shcherbakova, D.M. & Verkhusha, V.V. Near-infrared fluorescent proteins for multicolor *in vivo* imaging. *Nat. Methods* **10**, 751–754 (2013).
23. Riedl, J. *et al.* Lifeact: a versatile marker to visualize F-actin. *Nat. Methods* **5**, 605–607 (2008).
24. Muto, A., Ohkura, M., Abe, G., Nakai, J. & Kawakami, K. Real-time visualization of neuronal activity during perception. *Curr. Biol.* **23**, 307–311 (2013).
25. Apáti, Á. *et al.* Calcium signaling in pluripotent stem cells. *Mol. Cell. Endocrinol.* **353**, 57–67 (2012).
26. Wong, R.C., Pébay, A., Nguyen, L.T., Koh, K.L. & Pera, M.F. Presence of functional gap junctions in human embryonic stem cells. *Stem Cells* **22**, 883–889 (2004).
27. Hooper, R., Rothberg, B.S. & Soboloff, J. Neuronal STIMulation at rest. *Sci. Signal.* **7**, pe18 (2014).
28. LeDoux, J.E. Emotion circuits in the brain. *Annu. Rev. Neurosci.* **23**, 155–184 (2000).
29. West, A.E., Griffith, E.C. & Greenberg, M.E. Regulation of transcription factors by neuronal activity. *Nat. Rev. Neurosci.* **3**, 921–931 (2002).
30. Parekh, A.B. Store-operated CRAC channels: function in health and disease. *Nat. Rev. Drug Discov.* **9**, 399–410 (2010).

ONLINE METHODS

Plasmid construction. Expression plasmids for R-GECO1 and G-GECO1.0 (ref. 11) (Addgene plasmid #32444 and #32447, donated by R.E. Campbell, University of Alberta, Canada), LOVS1K (ref. 8) (Addgene plasmid #31981, donated by K. Truong, University of Toronto, Canada), Orai1-EYFP (ref. 31) (Addgene plasmid #19756, donated by A. Rao, La Jolla Institute for Allergy & Immunology, USA), msEGFP-PACR_pcDNA3 (ref. 7) (Addgene plasmid #55774, donated by T. Nagai, Osaka University, Japan), pLenti-CaMKIIα-ChETA-EYFP (ref. 32) and pLenti-CaMKIIα-hChR2(H134R)-EYFP-WPRE (ref. 33) (Addgene plasmid #26967 and #20944, donated by K. Deisseroth, Stanford University, USA), and piRFP670-N1 and piRFP682-N1 (ref. 22) (Addgene plasmid #45457 and #45459, donated by V. Verkhusha, Albert Einstein College of Medicine, USA) were obtained from Addgene. Sequence encoding codon-optimized Cry2 (amino acids 1–498, PHR domain)[34] was inserted into pEGFP-C1 (Clontech) after excision of *EGFP* by digestion with AgeI and BsrGI, to generate the Cry2-C1 vector. *EGFP* or *mCherry* cDNA flanked by NheI and AgeI sites was amplified by polymerase chain reaction (PCR) and inserted at the 5′ end of sequence encoding Cry2 to create EGFP-Cry2 or mCherry-Cry2 expression vectors, respectively. A nucleotide sequence for a flexible linker composed of 24 amino acids (three repeats of SGGGGGGG) was inserted at BsrGI and BspEI sites at the 3′ end of *EGFP* and *EGFP-Cry2* to generate EGFP-linker and EGFP-Cry2-linker expression vectors, respectively. Sequences encoding human STIM1 fragments (#1–#7, amino acids 238–685, 238–670, 238–501, 238–463, 238–416, 342–448 and 342–685) were PCR-amplified and ligated into the sequence encoding EGFP-Cry2-linker at BglII and EcoRI sites to create EGFP-Cry2-linker-STIM1ct variants. For construction of EGFP-Cry2(D387A)-linker-STIM1 (amino acids 238–685), sequence encoding Cry2(D387A) from construct encoding mCitrine-Cry2(D387A)-Vav2 (ref. 34), previously described, was PCR-amplified and ligated into sequence encoding EGFP-Cry2-linker-STIM1 (amino acids 238–685) at NruI and BspEI sites. R-GECO1$_{PM}$ was constructed by first PCR-amplifying sequences encoding R-GECO1 and then ligating them into pEGFP-C1 at NheI and BglII sites after excising the *EGFP* gene from the vector. Next, the sequence encoding the tail sequence of KRas4B (20 amino acids; KMSKDGKKKKKKSKTKCVIM) was fused to the sequence encoding the C terminus of R-GECO1 using an In-Fusion Cloning Kit (Clontech). Lastly, a sequence encoding a flexible linker (five repeats of the amino acid sequence SAGG) was PCR-amplified and inserted between sequences encoding R-GECO1 and the KRas4B tail at a BglII site. The NFATc1-mCherry expression vector was generated by replacing *GFP* cDNA in an NFATc1-GFP vector with PCR-amplified *mCherry* flanked by EcoRV sites. The sequence encoding NFATc1 was PCR-amplified and ligated into the piRFP682-N1 vector at NheI and AgeI sites to create NFATc1-iRFP682. The iRFP670-Lifeact expression vector was constructed by replacing mCherry of mCherry-Lifeact (ref. 34), previously constructed, into iRFP670 from piRFP670-N1 by AgeI and BsrGI sites. The sequence encoding mCherry was inserted into EGFP-Actin (Clontech) after excising EGFP with AgeI and BsrGI restriction enzymes to generate mCherry-Actin expression vector. For generating expression plasmid for EYFP-Orai1(E106Q), sequences encoding Orai1 was mutagenized through PCR-driven overlap extension using two mutagenic oligos (forward, 5′-AATGGTGCAAGTGCAGCTGGACGCTG ACC–3′ and reverse 5′-AGCTGCACTTGCACCATTGCCACCATGGCG-3′) and two flanking primers (forward 5′-GACTCTCGAGATGCATCCGGA GCCC-3′ and reverse 5′-GACTGAATTCGGGCATAGTGGCTGCCG-3′). The resulting PCR-amplified sequence encoding Orai1(E106Q) was cloned into XhoI and EcoRI of EYFP-N1 (Clontech). EGFP-tagged LOVS1K was generated by inserting PCR-amplified sequences encoding LOVS1K into EGFP-N1 (Clontech) at NheI and AgeI sites. Sequence encoding FKBP was PCR-amplified and inserted into previously constructed SNAP-Cry2-V_HH(GFP)[34] after excising sequence encoding SNAP-Cry2 at AgeI and BsrGI to create FKBP-V_HH(GFP) plasmid.

Cell culture and transfection. HeLa, NIH3T3, HEK293 and Cos-7 (ATCC) cells were maintained in Dulbecco's Modified Eagle's Medium (DMEM; PAA Laboratories GmbH) supplemented with 10% FBS (Invitrogen) at 37 °C in a humidified 10% CO_2 atmosphere. Human umbilical vein endothelial cells (HUVECs; Gibco) were maintained in Medium 200 (Gibco) supplemented with 2% low-serum growth supplement (Gibco) at 37 °C/5% CO_2. For HUVECs, plates were coated with 300 μg/ml of bovine collagen solution (PureCol; Advanced BioMatrix) for 1 h at 37 °C before plating. Astrocytes were prepared from 1–2-d-old C57BL/6 mouse pubs and were maintained in DMEM at 37 °C/10% CO_2. Hippocampal neurons were prepared from embryonic day 17–18 rats followed by Banker neuron culture[35], and then were dissociated with 0.25% trypsin and 10 mg/ml DNase. Neurons were seeded on a 96-well glass-bottom plate coated with 100 μg/ml poly(D-lysine) (Sigma). Glial cells were subsequently removed by treating with cytosine-1-b-D-arabinofuranoside (AraC; Sigma). Dissociated neurons were maintained in Neurobasal Medium supplemented with B27 (Invitrogen) and 2% FBS (GenDEPOT) at 37 °C/5% CO_2. Cells were transfected using either a Microporator (Neon Transfection System; Invitrogen) or Lipofectamine LTX (Invitrogen) according to the manufacturer's instructions.

siRNA transfection. Control or *Orai1* siRNA (Santa Cruz) diluted in siRNA Dilution Buffer (Santa Cruz) was transfected in each cell line plated on 60 mm dish through Lipofectamine LTX according to the manufacturer's instructions. For imaging dose-dependent attenuation of Ca^{2+} influx through OptoSTIM1 upon *Orai1* knockdown, HeLa cells transfected with 100 nM siControl or each diluted siRNA to Orai1 were collected at 24 h post transfection, subjected to electroporation with DNA encoding OptoSTIM1 and R-GECO1 through the microporator, and imaged at 48 h after siRNA transfection. For real-time reverse transcription (RT)-PCR, siRNA-transfected cells were prepared 48 h after transfection.

Live-cell imaging. For imaging, all cells were plated on 96-well glass-bottom plate (μ-Plate 96 Well ibiTreat; ibidi). Live-cell imaging was performed using a Nikon A1R confocal microscope (Nikon Instruments) mounted onto a Nikon Eclipse Ti body equipped with a Nikon CFI Plan Apochromat VC objective (60×/1.4 numerical aperture (NA); Nikon Instruments) and digital zooming of Nikon imaging software (NIS-element AR 64-bit version 3.21; Laboratory Imaging). A Chamlide TC system placed on a microscope stage was used for maintaining environmental conditions at 37 °C and either 5% or 10% CO_2 (Live Cell Instruments). Immediately before imaging, the medium was replaced with OPTI-MEM (Invitrogen) or neuronal imaging solution containing 145 mM NaCl, 2.5 mM KCl, 10 mM D-glucose, 10 mM HEPES, 2 mM $CaCl_2$ and 1 mM $MgCl_2$ for hippocampal neurons.

Whole-cell patch clamp recordings. HEK293 cells were cultured onto 6-well plates (SPL Life Sciences), transfected with OptoSTIM1 plasmid using Lipofectamine LTX (Invitrogen) and transferred onto coated 12-mm round coverslips (neuVitro) the next day. After 16 h, the coverslip was transferred onto a recording chamber. Successful transfection was confirmed through monitoring GFP expression under a fixed fluorescence microscope (Zeiss and Nikon). For whole-cell voltage-clamp recordings of I_{CRAC} in cells expressing OptoSTIM1, voltage stimuli consisting of a 50-ms step to −100 mV followed by a 45 ms voltage ramp from −100 to +80 mV were applied from the holding potential of 0 mV in every 5 s. The voltage ramp currents were continuously monitored and recorded until currents were stabilized under the continuous exposure of blue light (473 nm, 5 mW, CrystaLaser). Extracellular medium was replaced with $NMDG^+$–rich extracellular solution (150 mM $NMDG^+$) for assessing contribution of Na^+ currents in OptoSTIM1-mediated ramp currents. All data were present using a voltage ramp protocol and redrawn by leak subtraction. Recordings were carried out with a multiclamp 700B amplifier (Molecular Devices), filtered at 2 KHz and digitized at 10 KHz (Digidata 1440A and 1550, Molecular Devices). Recording pipettes (4–7 MΩ) were filled with intracellular solution (pH = 7.2, 280–290 mOsm) containing 140 mM Cesium-gluconate, 3 mM $MgCl_2$, 0.1 mM EGTA, and 10 mM HEPES, and 4 mM Mg-ATP with pH adjusted by CsOH. To avoid Ca^{2+} depletion-induced Ca^{2+} influx through CRAC channels, lower EGTA concentration was used. A transferred recording chamber was continuously perfused with extracellular solution (pH = 7.4, 310–320 mOsm) containing 140 mM NaCl, 5 mM CsCl, 10 mM HEPES, 10 mM $CaCl_2$, 1.2 mM $MgCl_2$, 20 mM glucose. Acquired data were analyzed using pCLAMP 10.4 (Molecular Devices). Access resistance (*Ra*, 10–35 MΩ) was continuously monitored. Data were discarded if *Ra* varied by >20% during recording.

Fura-2 imaging and calibration. Fura-2/AM (Invitrogen), dissolved in dimethyl sulfoxide, was diluted in DMEM at a final concentration of 2 μM, was loaded into HeLa cells at room temperature for 30 min. Fura-2 fluorescence was imaged using a Nikon A1R confocal microscope equipped with a 40×/0.75 NA CFI Plan Fluor objective and LAMBDA DG-4 lamp (Sutter Instrument Company) with excitation filters of 340 and 380 nm and an emission filter of 510 nm, and a Nikon DS-Qi1 monochrome digital camera. Intracellular $[Ca^{2+}]_{free}$ was calibrated and calculated according to the formula, $[Ca^{2+}]_{free} = K_d^{EGTA} \times (R - R_{min})/(R_{max} - R) \times F^{380}{}_{max}/F^{380}{}_{min}$, where K_d^{EGTA} is the dissociation constant of Fura-2, R_{min} and R_{max} are ratios at zero free Ca^{2+} and saturating Ca^{2+}, respectively, and $F^{380}{}_{max}$ and $F^{380}{}_{min}$ are fluorescence intensities with excitation at 380 nm for zero free Ca^{2+} and saturating free Ca^{2+}, respectively. K_d^{EGTA} was determined using a Fura-2 Calcium Imaging Calibration Kit (Invitrogen) according to manufacturer's instructions.

Imaging OptoSTIM1-induced Ca^{2+} influx. Different levels of Ca^{2+} influx presented in **Figure 1e** were induced by sequentially exposing cells to varying durations (1, 2.5, 0.5, 3.5, 1.5 and 4.5 s) of blue light at 15-min intervals. Transient and sustained Ca^{2+} influx was induced by stimulating cells at 12- and 3-min intervals, respectively. For experiments examining inhibition of Ca^{2+} influx through endogenous CRAC channels, cells were pretreated for 30 min with either 40 μM SKF96365 (Sigma) or 10 mM EGTA before imaging. For experiments using ionophore or Ca^{2+} store-depleting chemical to induce $[Ca^{2+}]_i$ elevation, 1 μM ionomycin (Sigma) or 10 μM thapsigargin (Sigma), respectively, was used. Photo-excitation was delivered using a photostimulation module in Nikon imaging software (NIS-element) that provided three loops of 0.5-s stimuli with 488 nm lasers. The light power density of 148 μW mm^{-2} (measured with an optical power meter from ADCMT) was used for photo-excitation, unless stated otherwise.

Structured illumination microscopy imaging. HeLa cells expressing OptoSTIM1 were scanned under a blue light (Intensilight C-HGFIE; Nikon Instruments) for 5 min. Cells were immediately fixed with methanol at −20 °C for 3 min and then rehydrated three times (5 min each) with 0.1% Triton X-100 in phosphate-buffered saline (PBS). After blocking with PBS containing 2% bovine serum albumin (BSA) and 0.1% Triton X-100, cells were incubated with a primary antibody against α-tubulin (1:1000; Sigma) for 20 min at room temperature and then washed three times. Cells were then incubated with Alexa Fluor 647–conjugated anti-mouse secondary antibody (Invitrogen) for 20 min at room temperature, and then imaged using a Nikon Structured Illumination Microscope (N-SIM; Nikon Instruments) equipped with a CFI SR Apochromat TIRF objective (100×/1.49 NA; Nikon Instruments).

Real-time RT-PCR analysis. Total RNAs were extracted from cell pellets through PureLink RNA Mini Kit (Invitrogen). cDNAs were reverse transcribed from total RNA samples using SuperScriptIII Reverse Transcriptase (Invitrogen). Gene expression was assessed using Bio-Rad CFX96 Touch Real-Time PCR Detection System with SYBR Green Realtime PCR Master Mix (TOYOBO). Data from each sample was normalized to the expression level of the gene encoding GAPDH and represented in delta C_T method[36]. Primers used for examining expression level of *Gapdh* and *Orai1* were (GAPDH-F 5′-GGAAGCTTGTCATCAATGGAA-3′, GAPDH-R 5′-TGGACTCCACGACGTACTCA-3′) and (Orai1-F 5′-ACCTCGGCT CTGCTCTCC–3′, Orai1-R 5′-GATCATGAGCGCAAACAGG-3′)[37].

p-CREB immunofluorescence. HeLa cells infected with lentivirus-delivered OptoSTIM1 were light illuminated using TouchBright W-96 LED Excitation System (Live Cell Instrument), in which LED power density corresponds to 0.7 mW mm^{-2} (470 nm) in our experimental condition, for 1 h in the 37 °C, 10% CO_2 incubator. Cells were then immediately fixed with 4% cold paraformaldehyde at room temperature for 20 min, and, after washing in PBST (PBS with 0.1% Tween-20), were subjected to blocking with PBS containing 0.3% TritonX-100 and 5% normal goat serum (Abcam) for 30 min. Primary antibody, Rabbit anti-p-CREB monoclonal antibody (1:2,000; Cell Signaling), was treated in PBS containing 0.1% TritonX-100 at 4 °C overnight. Cells were then washed in PBST and incubated with Alexa Fluor 594-conjugated goat anti-rabbit secondary antibody (1:2,000; Invitrogen) and Hoechst 33342 (1:10,000; Invitrogen) at room temperature for 1 h. After washing with PBST, cells were subjected to confocal imaging.

Zebrafish imaging. For neuronal expression of GCaMP7a in zebrafish, the neuron-specific GAL4 line, Tg[*huC*:Gal4-VP16], was crossed with Tg[*UAS*:GCaMP7a]. For mRNA synthesis, a pCS2+ expression vector containing sequences encoding either mCherry-STIM1(238–685) or mCherry-Cry2-STIM1(238–685) was linearized with NcoI, then transcribed using an mMESSAGE mMACHINE SP6 Transcription Kit (Ambion). The synthesized, capped mRNAs were dissolved in 0.2% phenol red and then microinjected into fertilized eggs at 20–30 pg/embryo. At 24 h after fertilization, embryos were anesthetized with tricaine (Sigma) and mounted on a 96-well glass-bottom plate coated with 3% methylcellulose (Sigma) for confocal imaging using a Nikon CFI Plan Apochromat VC objective (20 × 0.75-NA). Light stimulation was given by imaging with EGFP channel (488 nm, 1 mW mm^{-2}) at 10-s intervals for 5 min. All zebrafish experiments were approved by the Animal Ethics Committee of Chungnam National University (CNU 00393).

Viral vector construction and packaging. The pLenti-CaMKIIα-OptoSTIM1 plasmid was constructed by inserting PCR-amplified sequence encoding OptoSTIM1 into pLenti-CaMKIIα-ChETA-EYFP using BamHI and EcoRI sites after restriction of *ChETA-EYFP*. Sequences encoding *Ef1a* promoter was PCR-amplified and inserted into pLenti-CaMKIIα-OptoSTIM1 in exchange of *Camk2a* promoter at PacI and BamHI sites. *Camk2a* promoter–bearing OptoSTIM1 and ChR2 lentiviruses were packaged by the Penn Vector Core at the University of Pennsylvania, and *Ef1a* promoter–bearing OptoSTIM1 lentivirus was packaged by Cyagen Biosciences. The viral titers were 3.66×10^{11} and 4.73×10^{12} genome copies ml^{-1} for *Camk2a* promoter–bearing OptoSTIM1 and ChR2 viruses, respectively, and 3.54×10^{8} transduction unit ml^{-1} for *Ef1a* promoter–bearing OptoSTIM1 virus.

hESC culture and imaging. H9 human embryonic stem cells (WiCell Research Institute) were maintained on mitomycin C (MMC; A.G. Scientific)-treated mouse embryonic fibroblasts (MEFs) in the hESC medium (DMEM/F12 (Invitrogen) supplemented with 20% Knockout SR (Invitrogen), 1% non-essential amino acids (Invitrogen), 1% penicillin-streptomycin, 0.1 mM β-mercaptoethanol (Sigma), and 4 ng/ml FGF2 (R&D systems)). hESCs were dissociated by Accutase (Innovative Cell Technologies) and then infected with lentivirus encoding OptoSTIM1 under the control of *Ef1a* promoter. After infection, OptoSTIM1-positive hESCs were selectively isolated by using BD FACSAriaII (BD Biosciences) and further cultured in the hESC medium on MMC-treated MEF to stabilize OptoSTIM1 H9 hESCs. For image analysis, hESCs were placed on Matrigel (BD Biosciences)-coated 12-well glass-bottom plate (*In vitro* Scientific). X-Rhod-1/AM (Invitrogen), dissolved in Pluronic F-127 (Invitrogen), was diluted in the hESC medium at final concentration at 2 μM, was loaded into hESCs at 37 °C for 2 h. Live-cell imaging of hESCs was performed using a Nikon A1R confocal microscope with a Nikon CFI Plan Fluor objective (4×/0.13 NA) and a Nikon CFI Plan Apochromat objective (40×/0.95 NA). OptoSTIM1 in hESCs was activated using five loops of 120 ms duration of 488 nm laser at power density 5 mW mm^{-2} for spatial stimulation and three loops of 500 ms duration of 488 nm laser at power density 65 μW mm^{-2} for repeatable stimulation.

Animals. Behavioral experiments were performed on 12-wk-old male C57BL/6 mice purchased from Jackson Laboratory. Mice had free access to food and water and were kept on a 12-h light-dark cycle at 22 °C. All behavioral assays were conducted during the light phase of the light-dark cycle at the same time of day. All mice care and handling was performed according to the directives of the Animal Care and Use Committee of KAIST (Daejeon, Korea).

Stereotactic injection and optogenetic hippocampus stimulation. All surgeries were performed under stereotaxic guidance. Mice were anesthetized using 0.022 ml/g avertin. For optical stimulation of the CA1 region, OptoSTIM1 lentivirus was injected (coordinates relative to bregma: −2 mm anteroposterior; −1.25 mm mediolateral; −1.15 mm dorsoventral)[38,39] at a rate of 0.075 μl min^{-1} using a 10 μl Hamilton microsyringe (701N; Hamilton). After injection, the

doi:10.1038/nbt.3350

needle was left in place for 5 min before being slowly withdrawn. At 4 weeks, a 200-µm-core-diameter optic fiber (Doric Lenses) was implanted into the injection site for delivery of 473 nm laser light (7 mW, 20 Hz, 10 ms).

Behavioral analysis. Context A was a 20.5 × 19 × 30.5 cm conditioning chamber with a house light mounted directly above the chamber. The behavior of mice was recorded by digital video cameras mounted above the conditioning chamber. Digital video recordings were analyzed with FreezeFrame software (Actimetrics), which assesses freezing by measuring changes in the intensity of each pixel between successive frames of the video file. The conditioning procedure was conducted over 3 d. On day 1, mice were optically stimulated via the optic fiber for 25 min before conditioning. Afterward, mice were placed in context A and received paired stimuli of a tone (30 s, 90 dB, 3 kHz) and a co-terminating shock (2 s, 0.7 mA). The first tone presentation commenced 120 s after the mouse was placed in the chamber. There were three tone-shock pairings per session. The conditioned stimulus-unconditioned stimulus (CS-US) presentations were separated by a 120-s inter-trial interval during which immediate freezing was assessed. After the third CS-US presentation, mice were left in the chamber for an additional 90 s. The chamber was cleaned with 70% ethanol after each session. On day 2, mice were subjected to an almost identical procedure in the same context, except the CS was not presented. Freezing in this context was assessed over 5 min. The entire session was scored for freezing. On day 3, the context was modified to context B, which is a cylindrical chamber with white floor and walls scented with 40% diluted mouthwash. This chamber was used for testing conditioned fear in response to the tone in the absence of contextual cues. Each session lasted for 6 min. Freezing in the absence of the CS was assessed during the first 180 s of the test session, after which the CS was presented for 180 s and freezing was assessed. The investigator monitoring mice behavior was not blinded, but two other blinded investigators verified the reliability of the result. Sample sizes were not chosen to detect a prespecified effect size. Even though we did not use a method of randomization, we randomly selected mice for light stimulation among mice injected with OptoSTIM1. Statistical significance was evaluated using a paired two-tailed Student's *t*-test.

Histological processing and imaging. Mice were administered 0.022 ml/g avertin and euthanized by transcardial perfusion with 10 ml heparin (heparin natriumsalz; Carl Roth) followed by 10 ml of 4% paraformaldehyde in PBS. Brains were extracted and 40 µm coronal sections were cut on a cryotome. Then, sections were mounted on slides with Vectashield mounting medium with DAPI (Vector Laboratories). Images were captured using Zeiss LSM-780 confocal microscope (Zeiss) equipped with 20× objective lens.

Whole-cell patch clamp recording for brain slice. Mice were anesthetized and injected with either OptoSTIM1 or ChR2 lentivirus in CA1 region as described above. 3–4 weeks after virus injection, mice were anesthetized by avertin, and brains were isolated. The isolated brains in ice-cold artificial cerebrospinal fluid (ACSF; 125 mM NaCl, 2.5 mM KCl, 1.25 mM NaH_2PO_4, 25 mM $NaHCO_3$, 25 mM dextrose, 2 mM $CaCl_2$, 2 mM $MgCl_2$, 3 mM Na-pyruvate, 1 mM ascorbic acid, maintained at pH 7.4 by gassing with 95% O_2/5% CO_2) were sliced into 250 µm thick coronal sections using a Vibratome (VT-1200S; Leica). The slices were transferred to an incubation chamber filled with NMDG recovery solution (92 mM NMDG, 92 mM HCl, 30 mM $NaHCO_3$, 2.5 mM KCl, 0.5 mM $CaCl_2$, 10 mM $MgSO_4$, 1.2 mM NaH_2PO_4, 20 mM HEPES, 5 mM Na-ascorbate, 3 mM Na-pyruvate, 2 mM thiourea, 25 mM dextrose, maintained at pH 7.4 by gassing with 95% O_2, 5% CO_2) for 15 min at 36 °C. Then slices were maintained in oxygenated ACSF at room temperature for at least 1 h before use. CA1 neurons were recorded in oxygenated ACSF at 28–30 °C and visualized under an upright microscope (BX-51WI; Olympus) with IR-DIC and RFP optics. Whole-cell patch clamp recordings were performed using glass pipettes (3–4 MΩ) filled with internal solution (130 mM K-gluconate, 2 mM NaCl, 4 mM $MgCl_2$, 20 mM HEPES, 4 mM Na_2ATP, 0.4 mM Na_3GTP, 0.5 mM EGTA, pH 7.25, 290–295 mOsm). Light stimulation was delivered through optopatcher (2 ms, 20 Hz, 473 nm laser) (473 nm DPSS; SLOC) for 25 min under current-clamp at resting membrane potential. Afterward, current step was injected to confirm excitability of neurons. Access resistance was routinely monitored throughout the recordings, and data were excluded if the access resistance varied by more than 20% of the initial state or the holding current was not stable. All data were acquired with a multiclamp 700B amplifier (Molecular Devices), digitized at 1 kHz with an A-D converter (Digidata 1550; Molecular Devices), and analyzed using Clampfit (Molecular Devices).

Image processing and analysis. Images were analyzed using Nikon imaging software (NIS-element AR 64-bit version 3.21; Laboratory Imaging). Changes in fluorescence intensities of R-GECO1, R-GECO1$_{PM}$, NFATc1-iRFP682, and iRFP670-Lifeact were quantified using the 'Time Measurement' tool. For quantifying changes of R-GECO1 intensity during OptoSTIM1 activation, cells with initial intensity of R-GECO1 between 100 and 500 (a.u.) were selected to be analyzed. For all fluorescence intensities from a single image were measured using the 'Annotations and Measurements' tool. Kymographs for Lifeact and R-GECO1 were drawn by the 'Create Kymograph by Line' tool. Assessment of $T_{1/2}$ values has been previously described[40]. For acquiring maximal intensity-projected image, recorded movie was subjected to the 'Maximum Intensity Projection' tool. Protrusion/Retraction Map of NIH3T3 cell was obtained as previously described[34]. Statistical significance was evaluated using a two-tailed Student's *t*-test.

31. Prakriya, M. *et al.* Orai1 is an essential pore subunit of the CRAC channel. *Nature* **443**, 230–233 (2006).
32. Gunaydin, L.A. *et al.* Ultrafast optogenetic control. *Nat. Neurosci.* **13**, 387–392 (2010).
33. Zhang, F. *et al.* Multimodal fast optical interrogation of neural circuitry. *Nature* **446**, 633–639 (2007).
34. Lee, S. *et al.* Reversible protein inactivation by optogenetic trapping in cells. *Nat. Methods* **11**, 633–636 (2014).
35. Kaech, S. & Banker, G. Culturing hippocampal neurons. *Nat. Protoc.* **1**, 2406–2415 (2006).
36. Schmittgen, T.D. & Livak, K.J. Analyzign real-time PCR by the comparative C_T method. *Nat. Protoc.* **3**, 1101–1108 (2008).
37. Chin-Smith, E.C., Slater, D.M., Johnson, M.R. & Tribe, R.M. STIM and Orai isoform expression in pregnant human myometrium: a potential role in calcium signaling during pregnancy. *Front. Physiol.* **5**, 169 (2014).
38. Goshen, I. *et al.* Dynamics of retrieval strategies for remote memories. *Cell* **147**, 678–689 (2011).
39. Tsutajima, J., Kunitake, T., Wakazono, Y. & Takamiya, K. Selective injection system into hippocampus CA1 via monitored theta oscillation. *PLoS ONE* **8**, e83129 (2013).
40. Kim, N. *et al.* Spatiotemporal control of fibroblast growth factor receptor signals by blue light. *Chem. Biol.* **21**, 903–912 (2014).